Relating ^{137}Cs and sediment yield from uncultivated catchments: the role of particle size composition of soil and sediment in calculating soil erosion rates at the catchment scale

P. Porto[1,2] · G. Callegari[2]

Abstract

Purpose Soil loss is considered one of the most important consequences of land degradation as it affects the production of agricultural and forested areas, and the natural equilibrium of aquatic ecosystems downstream. For these reasons, the availability of tools and techniques able to identify areas at risk of land degradation is essential. Over the last 3–4 decades, theoretical models, based on the use of ^{137}Cs, an anthropogenic radiotracer, proved to be very effective for this purpose. However, these models require specific information on soil and sediment particle size to provide estimates of soil erosion or deposition and this information is summarised by a particle size correction factor 'P'. Empirical methods of calculation of this factor assume the basic hypothesis that a particle size selectivity takes place in erosion processes and this results in a general enrichment of the fine component in sediments and a corresponding higher radionuclide activity. In this contribution, we demonstrate that this hypothesis is not valid everywhere, and consequently, the P factor cannot be estimated using traditional approaches.

Materials and methods A long-term experiment, conducted in Southern Italy and based on two small experimental catchments (approximately 1.5 ha in size), for which measurements of sediment yield are available for the period 1978–2020, is used in this work. More specifically, ^{137}Cs measurements carried out within the catchments and on a reference area provided the basis to obtain long-term estimates of soil erosion rate in these sites. Combined measurements of ^{137}Cs activity and particle size on both soils and sediments, obtained for 46 events, were also carried out to explore possible particle size effects on the final estimates of soil loss.

Results and discussion Particle size analyses of soil and sediments showed that there is evidence of a general enrichment of the eroded soil in the finer size fractions. Conversely, radiometric analyses revealed that ^{137}Cs activity in sediments is generally lower than that in surface soil. These results reflect both the decreasing ^{137}Cs activity associated with depth in undisturbed soils and the higher specific surface area of the deeper horizon in these soils. These findings preclude the application of the available empirical models to calculate P, and suggest the opportunity to use, for long-term estimates of soil erosion, a particle size correction factor $P = 1$. This assumption and an uncertainty analysis associated with the spatial variability of the ^{137}Cs reference value were incorporated into the Diffusion and Migration Model (DMM) to obtain estimates of soil erosion rates for the study catchments.

Conclusions The final estimates of soil erosion provided by the DMM showed values very close to the measurements of sediment yield obtained for the two catchments during the study period. The overall results demonstrated that the DMM, if properly calibrated using specific information of particle size and of ^{137}Cs reference value, can be considered a useful tool to individuate areas more prone to risks of land degradation and to identify appropriate strategies able to reduce soil loss in forested sites.

Keywords Soil erosion · Experimental catchments · ^{137}Cs · Particle size selectivity · Model validation · Southern Italy

Responsible editor: Cédric Legout.

Extended author information available on the last page of the article

1 Introduction

Soil loss is considered one of the most important consequences of land degradation in many countries of the world as it affects the production of agricultural and forested areas (see Panagos et al. 2018), and may cause drastic changes in the natural equilibrium of aquatic ecosystems downstream (Wood and Armitage 1999; Heywood and Walling 2007). In recent decades, the magnitude of soil erosion is increasing worldwide due to the combined effects of land abandonment (Romero-Díaz et al. 2017), anthropic activities (Nearing et al. 2017; Manojlović et al. 2018) and climate change (Porto et al. 2022). A general effort to quantify soil loss was made in many countries (e.g. Cerdan et al. 2010; Maetens et al. 2012). To date, experiments dealing with soil erosion measurements on small experimental areas are available at a global scale and these data are used to calibrate and validate prediction models to identify areas at higher risk (see Cerdan et al. 2010; Maetens et al. 2012). The utility of similar studies is certainly recognised, but the difficulty to extrapolate the results in larger areas where no direct measurements are available suggested the need to explore alternative methods.

During the last 3–4 decades, the use of caesium-137 (^{137}Cs) proved to be a valid alternative to traditional methods as it provided reliable estimates of soil erosion both at plot (Kachanoski 1987; Porto and Walling 2012; Zhang 2018) and at catchment scale (Porto et al. 2001, 2018). The fallout radionuclide ^{137}Cs (with a half-life of approximately 30 years) is associated with the testing of nuclear weapons occurring from the late 1950s to the early 1960s (Zapata 2002; Ritchie and Ritchie 2005; International Atomic Energy Agency 2014). The successful application of this technique is based on a simple comparison between the inventory values obtained in single sampling points established in the area under investigation and a so-called '^{137}Cs reference value' obtained in non-eroded sites at time of sampling. This technique offers many advantages that include its relative simplicity (Zapata 2002; IAEA 2014), the possibility to obtain retrospective information of soil redistribution rates (Walling and Quine 1992; Mabit et al. 2008), the ability to get a spatial distribution of the estimates derived from single sampling points (Mabit et al. 2009; Zhang et al. 2019), the chance to provide sediment budgets for large areas (Campbell et al. 1988; Belyaev et al. 2013; Minella et al. 2014; Navas et al. 2014), the opportunity to calibrate and validate empirical and theoretical soil erosion models based on both lumped and distributed approaches (Walling and He 1998; Porto and Walling 2015; Zhang 2017) and the possibility to explore the effects on soil erosion produced by changes in land

use (Moustakim et al. 2019), cultivation techniques (Lobb et al. 1995; Li et al. 2010), silvicultural treatments (Porto et al. 2009; Altieri et al. 2018) and environmental disturbances like wildfires (Wilkinson et al. 2009; Owens et al. 2012; Estrany et al. 2016; Porto and Callegari 2021).

There is, however, one important limitation associated with this technique that needs attention. It includes the choice of a conversion model able to convert loss or gain of ^{137}Cs into estimates of soil erosion or deposition. Even if empirical models were proposed (e.g. Elliott et al. 1990; Ritchie and McHenry 1990; Walling and Quine 1990; Loughran and Campbell 1995), their use is questionable because they are limited to local contexts. To date, attention is focused on theoretical models (different for cultivated and uncultivated sites) that, in view of their ability to interpret the variation of ^{137}Cs activity along a soil profile, should provide reliable estimates of soil redistribution rate (Yang et al. 1998; Walling and He 1999; Porto et al. 2003a). However, the validity of such approaches is strongly dependent on the assumptions incorporated into the models and some of these assumptions are difficult to test for several reasons. The first reason is related to the lack of long-term measurements of soil loss available for a time window comparable with that covered by the ^{137}Cs measurements. This makes the comparison between measurements and estimates of soil erosion difficult and, in this respect, only a few contributions are available in the literature (Kachanoski 1987; Porto et al. 2004, 2018; Zhang 2018). The second reason concerns the absence of specific studies aimed at validating the robustness of the calibration parameters incorporated into the models. For example, many researchers have emphasised the need to incorporate into the conversion models a specific parameter, P, that accounts for the grain size selectivity of erosion processes (e.g. Walling and Quine 1990; Sutherland 1991; Walling and He 1999; Porto et al. 2003a). In fact, possible contrasts in grain size composition of sediment relative to the surface soil will influence its ^{137}Cs content and, consequently, the estimates of soil erosion may be biased. Based on this premise, if it is assumed that the ^{137}Cs concentration of sediment is similar to that of the surface soil, i.e. preferential mobilisation of the finer fractions is neglected, the rates of soil erosion will be overestimated. Equally, if the ^{137}Cs activity of sediment is less than that of the surface soil, i.e. preferential mobilisation of the coarser fractions is assumed, erosion rates will be underestimated. However, even if the enrichment in fines of sediment, due to preferential mobilisation of the finer particles of primary soils, has been recognised in the literature (e.g. Stone and Walling 1997; Mabit and Blake 2019), other researchers document the opposite (i.e. the eroded soil is coarser than the surface soil) especially when the transport processes involved are dominated by rainsplash erosion (see Young and Onstad 1978; Young

1980; Porto et al. 2003b). These findings suggest that it is difficult to provide suitable estimates of a particle size factor if the long-term dynamic of the transport processes involved is unknown. To date, only empirical approaches are available to account for particle size effect in ^{137}Cs concentration of sediment and primary soil and these are used to provide estimates of P in the conversion models (He and Walling 1996; Taylor et al. 2014). However, these approaches are based on particle size data of sediment and primary soil obtained from experiments of limited duration and no specific tests have been conducted when long-term estimates of soil erosion are needed.

Another source of uncertainty associated with the use of ^{137}Cs conversion models is related to the spatial variability of the ^{137}Cs inventories (both in the study areas and in the reference location) that can be altered by the presence of trees (fallout interception) and/or by possible additional fallout caused by nuclear accidents (Chernobyl and/or Fukushima) (Zapata 2002; Barsanti et al. 2012). This aspect is often overlooked or ignored in many studies and it can lead to erroneous estimates of the ^{137}Cs reference value and, consequently, to biased estimates of erosion and deposition rates (IAEA 2014).

This paper reports an analysis of the relationships between ^{137}Cs loss and sediment yield from two catchments located in Southern Italy. This analysis demonstrates that the spatial variability of the ^{137}Cs atmospheric fallout and the uncertainty related to the particle size effect can be incorporated into a conversion model to provide long-term estimates of soil erosion at the catchment scale.

2 Material and methods

2.1 The experimental catchments W2 and W3

The study catchments W2 and W3 have drainage areas of 1.38 and 1.65 ha, respectively. They are two sub-catchments of the larger Crepacuore basin (18.2 km^2) that drains to the Jonian Sea approximately 5 km north of Crotone (39°04′50″N, 17°07′38″E) in Calabria, Southern Italy (Fig. 1). The catchments are located at Brasimato (39°07′52″N, 17°01′36″E) over an area that, geologically, is incised into the Upper Pliocene and Quaternary clays, sandy clays and sands and shows a soil texture made up of a silt–clay content of approximately 86% for the catchment W2 (Di Stefano et al. 2005) and approximately 79% for the catchment W3 (Porto et al. 2003a). The values of the mean slope are approximately 35% for catchment W2 and 24% for catchment W3. The climate of this area experiences large seasonal fluctuations with most of the precipitation occurring from October to March and concentrated in a few large events that account for more than 50% of the annual value

(Porto and Callegari 2019). Based on the data collected at the near station of Crotone (39°04′45″N, 17°07′00″E), the mean annual rainfall related to the period 1916–2020 is approximately 664 mm whilst the mean annual air temperature related to the period 1925–2020 is approximately 17.3 °C.

The catchments W2 and W3 have never been under cultivation and originally they supported a rangeland vegetation cover consisting mainly of *Aegylops ovata*, *Atriplex halimus*, *Lepturus cylindricus* and *Lygeum spartum*. In 1968, both the catchments were afforested with eucalyptus trees (*Eucalyptus occidentalis* E.) in order to (a) reduce soil erosion in this region and (b) expand the forested area in Calabria to increase wood production. However, the result of the afforestation was not completely successful as the tree cover within catchment W2 is discontinuous with about 20% of the drainage area, mostly in the hillslopes facing south, characterised by the absence of trees with a sparse grass cover. In these areas, the absence of vegetation caused the formation of several rills (see Fig. 2) that can be expected to mobilise sediment from lower in the soil profile. A previous investigation made by Porto et al. (2005) suggested that most sediment collected at the catchment outlet could originate from these areas, emphasising the importance of vegetation cover in influencing sediment mobilisation from the study catchment. In catchment W3, the eucalyptus cover is more uniform with only about 3–4% of the drainage area covered by grass, and a few rills have occurred in these small areas (see Fig. 2).

In 1978, a national 'Project on Soil Conservation' (Porto and Callegari 2021) was launched to monitor the effects of soil erosion in the country and these two catchments were included in the long-term monitoring programme. For this purpose, these two experimental catchments were equipped to provide specific information on rainfall, runoff and sediment yield in Southern Italy. More specifically, rainfall is measured with a mechanical rain gauge located in the upper part of each catchment and runoff is measured with an H-flume weir (Brakensiek et al. 1979) coupled with a mechanical stream gauge located at the catchment outlet. The stream gauge (see Fig. 2 for details) provides measurements of runoff based on a calibrated stage-discharge relationship (Parson 1954; Brakensiek et al. 1979). Sediment yield records are provided using a Coshocton Wheel placed downstream the H-flume and coupled with two sized tanks that collect the portion of runoff that is intercepted by the sampler. The Coshocton Wheel (Fig. 2) was built according to Parson (1954) and Carter and Parson (1967) and it was calibrated in 1978 with the use of a tank truck by pumping a known amount of water to the flume. Several tests, made before the beginning of the experiments, indicated that the device collects a sample of approximately 1/200 of the total flow volume measured by the stream gauge. Considering the very small size of the transported soil particles and the
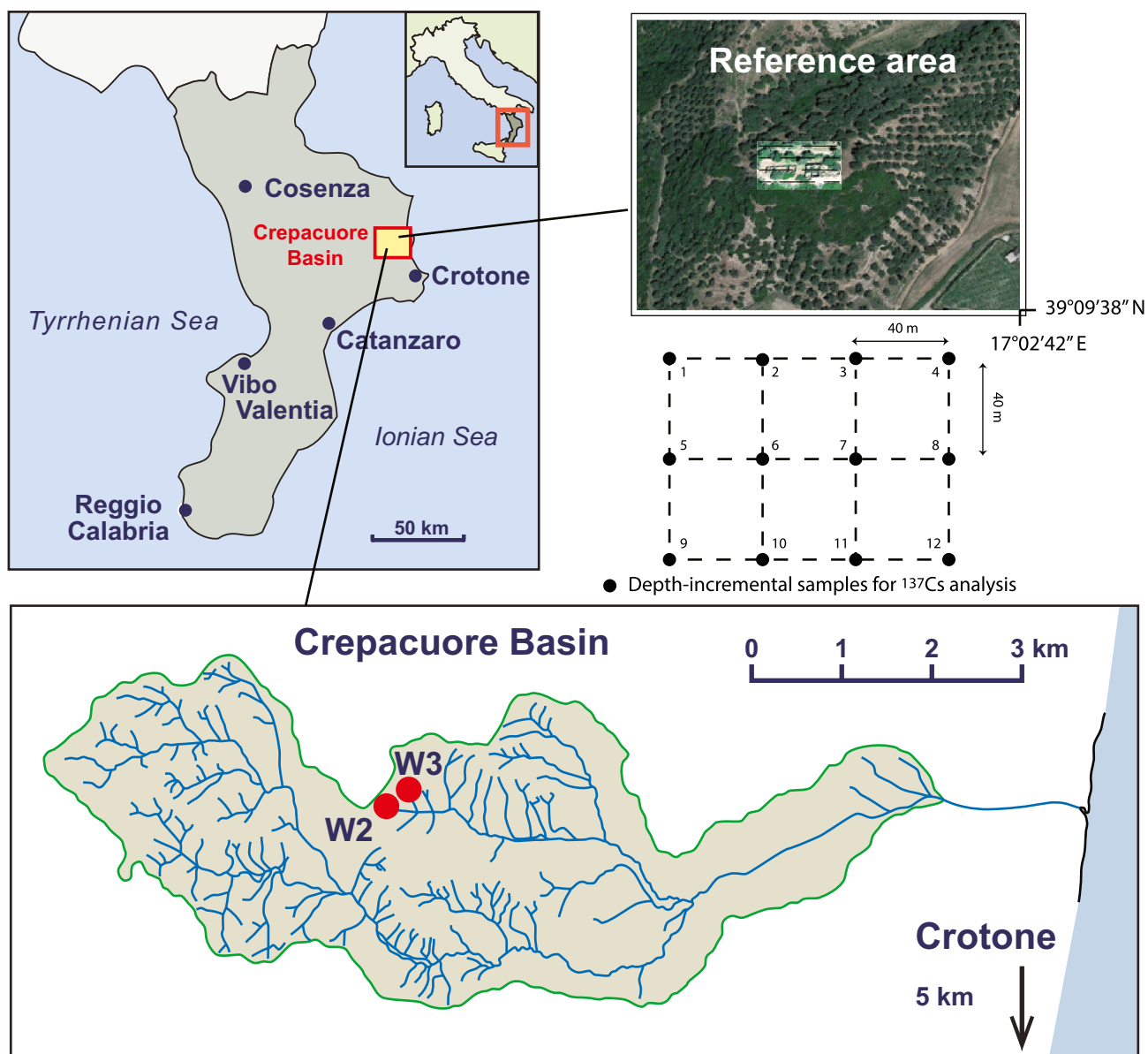
Fig. 1 The study area: location of the experimental catchments W2 and W3 and of the reference area selected to establish the ^{137}Cs baseline

functioning operation of the Coshocton-type sampler, the device collects all particle classes of the sediment that passes through the outlet with no distinction between bed and suspended sediment load. This allows a direct comparison between sediment and soil properties in these catchments. Measures of rainfall, runoff and sediment yield are generally obtained at event scale. However, when short-time interval occurred between two or more consecutive events, only one measurement of sediment yield was possible and the corresponding data of rainfall and runoff responsible for that sediment output were aggregated accordingly. The sediment output for each event (or cumulated events) is calculated by multiplying the mean sediment concentration measured at

the tanks times the corresponding runoff volume provided by the stream gauge. The annual sediment yield is then obtained by the sum of the sediment output related to the erosive events which occurred in that year.

2.2 Soil and sediment sampling and laboratory analyses

Collection of soil samples involved three separate sampling campaigns. The first campaign was undertaken in February 2021 within the catchment W2 and a total of 55 sampling points were established based on the grid shown in Fig. 2. This sampling exercise involved the collection
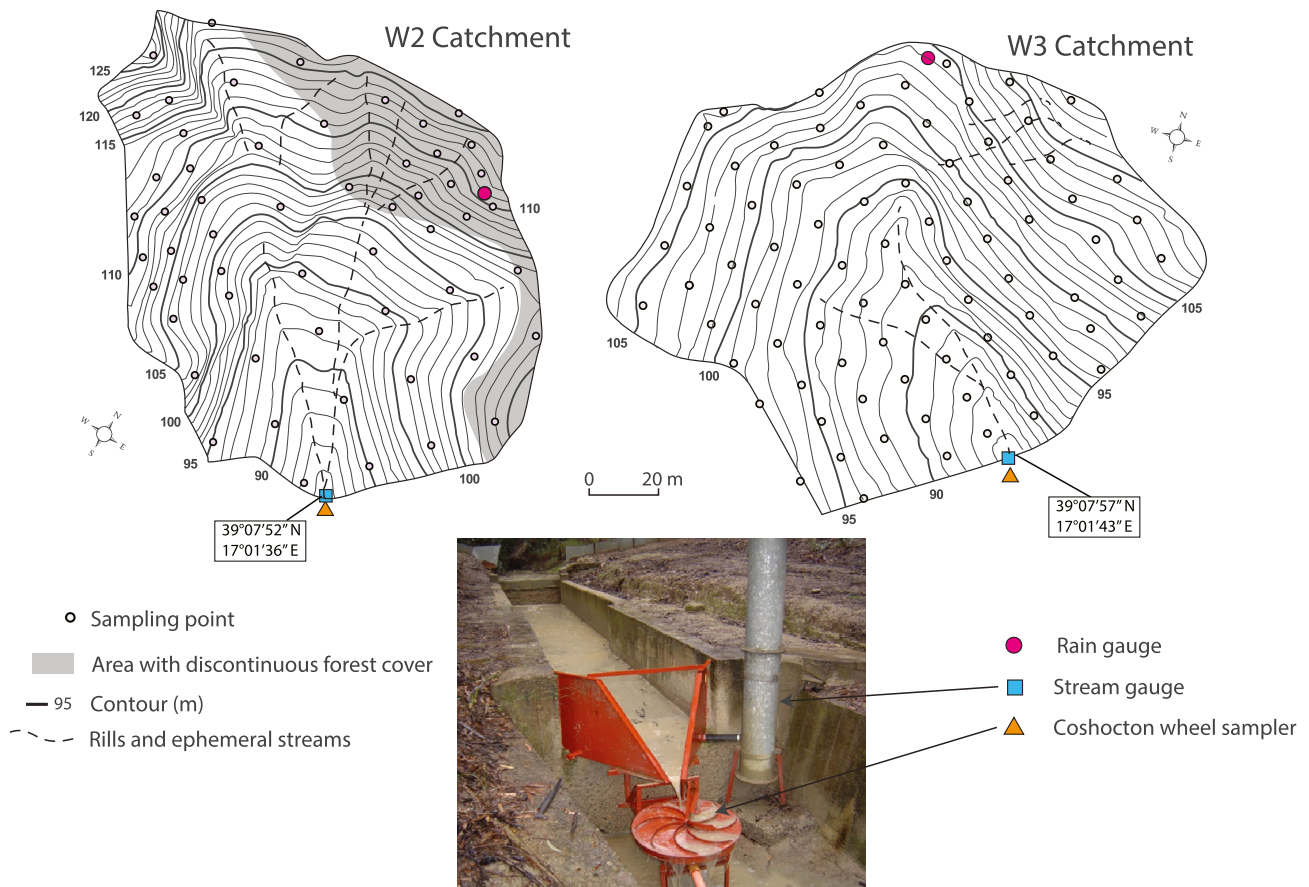
Fig. 2 The study catchments, the measurements device and the sampling locations. The location of the areas with scarce vegetation and the presence of rills are also indicated for the study catchments

of representative samples of soil at two different depths (0–1 cm and 1–15 cm) for particle size analyses and measurements of ^{137}Cs activity, and the collection of two bulk cores (at a depth of 0–15 cm) for measurements of ^{137}Cs inventories. A number of additional 45-cm cores was collected and sectioned into 15-cm depth increments, in order to confirm that no ^{137}Cs content was detectable below the depth of 15 cm (Porto et al. 2014). Because the eucalyptus trees were planted in 1968 when most of ^{137}Cs atmospheric flux had already reached the soil, we assumed that fallout interception was minimal during the period covered by the trees and the spatial variability of ^{137}Cs inventories around the sampling points is very low. However, the samples were collected 2–3 m distant from the tree trunks, and in small clearings under the trees in order to avoid problems due to stemflow and the two bulk cores served to minimise canopy interception effects.

Soil samples related to the depth of 0–1 cm, consisting of three samples for each sampling point, were taken using a square wooden frame (10×10 cm^2). The three samples were analysed separately for ^{137}Cs activity and particle size distribution. The mean value for each sampling point served

to compare ^{137}Cs content of soil surface with that of the sediment collected at the catchment outlet; samples collected at a depth of 1–15 cm (taken using the same frame) were used to compare the particle size distributions related to different soil layers. The two bulk cores, collected at a depth of 0–15 cm for measurements of ^{137}Cs inventories, were merged for each sampling point in order to account for spatial variability and to reduce the number of samples to be analysed.

The second sampling campaign was carried out for the catchment W3, in March 2021. The same sampling strategy was used and involved the selection of 81 sampling points (see Fig. 2). Again, three soil samples at two different depths (0–1 cm and 1–15 cm) were collected for each sampling point for particle size analyses and measurements of ^{137}Cs activity. Contextually, two bulk cores were also taken (at a depth of 0–15 cm) for each sampling point for measurements of ^{137}Cs inventories. The two bulk cores collected for each sampling point were merged.

The third sampling campaign was designed to provide details on the ^{137}Cs reference value. In this case, a detailed sampling strategy was followed to account for spatial

variability of the ^{137}Cs fallout and to detect possible additional flux from Chernobyl in the area. The ^{137}Cs fallout due to the Fukushima accident was extremely low in Italy (Barsanti et al. 2012) and it was not considered in our calculations.

Details of the sampling strategy in the reference area are reported in a recent paper (Porto and Callegari 2022) in which the temporal distribution of ^{137}Cs fallout was reconstructed based on the previous analyses carried out by Porto et al. (2001, 2003a, b, 2016, 2018) and on the temporal fallout record provided at national scale (ISIN 2021). In brief, this sampling campaign, undertaken in March 2021, involved the selection of a larger stable area (approximately 1 ha in size) in which the collection of 12 sectioned cores following a regular grid scheme was undertaken (see Fig. 1). The cores were taken using a sampling device consisting of a motorised soil column cylinder auger set in which a core tube with internal diameter of 11 cm is accommodated. Each sample was sectioned into increments of 2 cm and was analysed separately for ^{137}Cs content. All samples were dried and sieved to < 2 mm prior to particle size and ^{137}Cs analyses.

Collection of sediment samples involved a total of 92 samples associated with 46 storm events occurring, in each catchment, during the period from November 2013 to November 2020. In this case, the sediment samples were collected from the storage tanks associated with the Coshocton wheel samplers at the outlet of catchments W2 and W3. Again, the samples were dried and sieved to < 2 mm prior to particle size and ^{137}Cs analyses.

A standard procedure for preparing soil samples for particle size analysis was followed and it consisted of pretreatment with hydrogen peroxide to remove the organic component and dispersion with sodium hexametaphosphate and ultrasonic bath. The remaining sediment–water mixture was centrifuged at 3000 rpm for 30 min and the supernatant decanted. The pre-treatment phase required approximately 4–6 days, depending on the organic component, and it allowed a complete dispersion of the soil particles. Subsequently, the size distribution of the samples was determined using the Analysette 22 MicroTec plus (Fritsch) laser diffraction device with the measuring range from 0.08 μm up to 2 mm. The method is based on the light scattered at different angles by the particles as they pass through a laser beam. In our analyses, the Fraunhofer algorithm was used with a beam obscuration of approximately 13%. The specific surface area (*SSA*) of each sample (m^2 g^{-1}) was estimated from its grain size distribution, assuming spherical particles.

Radiometric analyses to determine ^{137}Cs activity were made on the sediment samples collected from the catchment outlets, on the representative samples of surface soil (0–1 cm), on the sectioned and soil bulk cores (0–15 cm) collected within the catchments and on the sectioned cores obtained in the reference area. The samples were measured by two Canberra p-type high-resolution low-energy coaxial HPGe detectors (model GX4020) with a relative efficiency of approximately 45%. The Canberra Genie 2000 software package was used to perform the spectral analysis. More specifically, a Monte Carlo procedure, associated with the Canberra's LabSOCS (Laboratory SOurceless Calibration Software) code and able to establish the calibration efficiency for any type of geometry, was preliminarily performed for each detector. The energy calibration was obtained using a certified ^{155}Eu and ^{22}Na multigamma source with a wide energy range (42.8–1274.5 keV). Subsequently, a validation phase was performed using the activity concentration for ^{137}Cs of standard materials presented to the detectors in containers of identical geometry to those used for the study (Petri dishes or Marinelli beakers). The standards were produced by adding a measured amount of certified liquid standard to a known amount of < 2-mm soil with a ^{137}Cs activity below the level of detection and representative of the samples to be analysed. This operation was repeated for each detector and the two types of equipment did not show substantial differences in terms of efficiency. The background noise of the detection system was also evaluated using blank samples of identical geometry in order to improve the accuracy of the measurement. Counting time varied from approximately 80,000 to approximately 240,000 s depending on the activity that was expected for each sample. The above procedure provided final results with an analytical precision of approximately 10% at the 95% level of confidence. The lower limit of detection depends on efficiency and counting time, and thus, it differs from sample to sample. The activity (Bq kg^{-1}) for each sample was obtained from the counts at the 662-keV peak in the measured γ-ray spectrum. The inventory (Bq m^{-2}) of each bulk core was calculated as the product of the measured ^{137}Cs activity (Bq kg^{-1}) and the dry mass of the < 2-mm fraction of the bulk core (kg), divided by the surface area of the core (m^2). The total inventory corresponding to the sectioned cores (Bq m^{-2}) was obtained in turn by summing the above product (Bq) of all layers, into which the core was sectioned, divided by the surface area of the core (m^2).

2.3 The conversion model used to convert ^{137}Cs loss into soil erosion rates for the two catchments

The amount of soil eroded from each catchment depends on the degree ^{137}Cs depletion that has occurred during the period covered by the ^{137}Cs measurements. To this purpose, a conversion model, able to quantify the degree of reduction of the

measured inventory, relative to the local reference inventory, is necessary. The conversion model used in this work is the Diffusion and Migration Model (DMM), in the refined version proposed by Porto et al. (2003a). This version of the DMM is based on a simulation of the ^{137}Cs activity along a soil profile following measured records of the atmospheric fallout and its temporal redistribution. Based on this premise, the DMM attempts to reproduce the activity of ^{137}Cs, for a single value of mass depth x and time t', with the following equation:

$$C(x,t,t') = e^{-\lambda(t-t')} \int_0^\infty \frac{I(t')}{H} e^{-\frac{y}{H}} \left\{ e^{\frac{V(x-E-y)}{2D} - \frac{V^2(t-t')}{4D}} \left[e^{-\frac{(x-E+y)^2}{4D(t-t')}} + e^{-\frac{(x-E-y)^2}{4D(t-t')}} \right] \right.$$

$$\left. \times \frac{1}{\sqrt{4\pi D(t-t')}} - \frac{V}{2D} e^{\frac{Vx}{D}} erfc \left[\frac{x - E + y + V(t-t')}{\sqrt{4D(t-t')}} \right] \right\} dy \tag{1}$$

where $C(x,t,t')$ (Bq kg^{-1}) represents the ^{137}Cs activity simulated for a single value of mass depth x and time t'; $I(t')$ expressed in (Bq m^{-2} yr^{-1}) indicates the ^{137}Cs amount of fallout that has reached the ground at time t' (year); H (kg m^{-2}) is a constant that represents the ^{137}Cs initial relaxation mass depth; D (kg^2 m^{-4} yr^{-1}) is a diffusion coefficient, assumed constant in time and space; V (kg m^{-2} yr^{-1}) is a migration coefficient representing the constant downward migration rate; λ (= 0.023 yr^{-1}) is the constant of radioactive decay for ^{137}Cs; x (kg m^{-2}) indicates the cumulative mass depth; t (year) is the time elapsed since the commencement of fallout in 1954; E (kg m^{-2}) indicates a constant rate of lowering of the soil surface by erosion ($E = 0$ for a reference profile); and erfc(u) is the error-function complement defined as (Crank 1975)

$$erfc(u) = \frac{2}{\sqrt{\pi}} \int_u^\infty e^{-y^2} dy \tag{2}$$

At first, Eq. (1) is integrated for each value of x using a fixed value of t' and a soil layer of variable thickness y (here expressed in kg m^{-2} as a mass length) for which a diffusional transport in a water-saturated porous medium is assumed (Lindstrom and Boersma 1971; Pegoyev and Fridman 1978). Then, in order to get the total value of ^{137}Cs concentration $C(x,t)$ (Bq kg^{-1}) for that value of x, it is necessary to account for the fallout input occurred from 1954 to the date of sampling. This will be obtained by integrating Eq. (2) over time t', assuming a continuous input $I(t')$ viz:

$$C(x,t) = \int_0^t C(x,t,t') dt \tag{3}$$

The attempt of Eq. (3) to simulate the diffusion and migration of ^{137}Cs along the soil column was demonstrated in several works carried out in southern Italy (see Porto et al. 2004, 2016; Altieri et al. 2018) and in UK (see He and Walling 1997).

3 Results

3.1 The sediment yield measurements

The long-term monitoring of the two study catchments W2 and W3, related to the study period 1978–2020, provided the two datasets of annual sediment yield illustrated in Fig. 3. The figure shows also the amounts of rainfall and runoff related to the sediment yield values. The missing values in Fig. 3, corresponding to the years 1981, 1988 and 1989 for the catchment W2, are related to absence of observations because the device did not work properly for the events that occurred in those years. Consequently, those three years were discarded from the overall analyses. The same occurred for the period 1995–2005 during which both the catchments W2 and W3 did not work for budget problems. The experiments re-started at the end of 2005, when the devices were refurbished, and they are still working without interruption.

Since the beginning of the experiment, logging operations were conducted in each catchment in order to evaluate the effectiveness of the canopy cover on soil loss, to monitor the long-term effect of afforestation on soil protection and to quantify the production of the eucalyptus plantation. More specifically, the trees in the catchment W2 were cut in 1978 and in 1990. The cutting operations took place across the entire area of the catchment and involved the removal of approximately 30–40 m^3 of biomass during each logging campaign. The harvested timber was extracted from the catchment manually, in order to minimise the impact on the soil surface. From 1990 to date no silvicultural treatments were applied in this catchment and the condition of trees was maintained more or less stable even if recent tree mortality related to an attack of *Phoracantha semipunctata* (a species of beetle originating from Australia) caused a number of single trees to fall down. In the catchment W3, the trees were cut every 10 years since 1986, mainly for wood production. After cutting the trees regrow naturally in each catchment. However, the spatial distribution of the trees in catchment W2 is discontinuous and approximately 20% of the total area is covered by natural grasses (see Porto et al. 2009). In catchment W3, the forest cover is well developed and the presence of grass combined with sparse trees is limited to approximately 3–4% of the total area. The logging operations applied to these catchments caused the exposure of soil to the rainfall impact, and this affected the temporal variability of the measurements shown in Fig. 3. This variability of sediment production reflects also the seasonal regime of the rainfall, characterised by the occurrence of frequent flash floods, and the alternate dominance of soil erosion processes (rill and interrill) due to the different magnitude of the erosion processes. For example, the high values of sediment yield obtained for the catchment W2 in 1990 and 1992
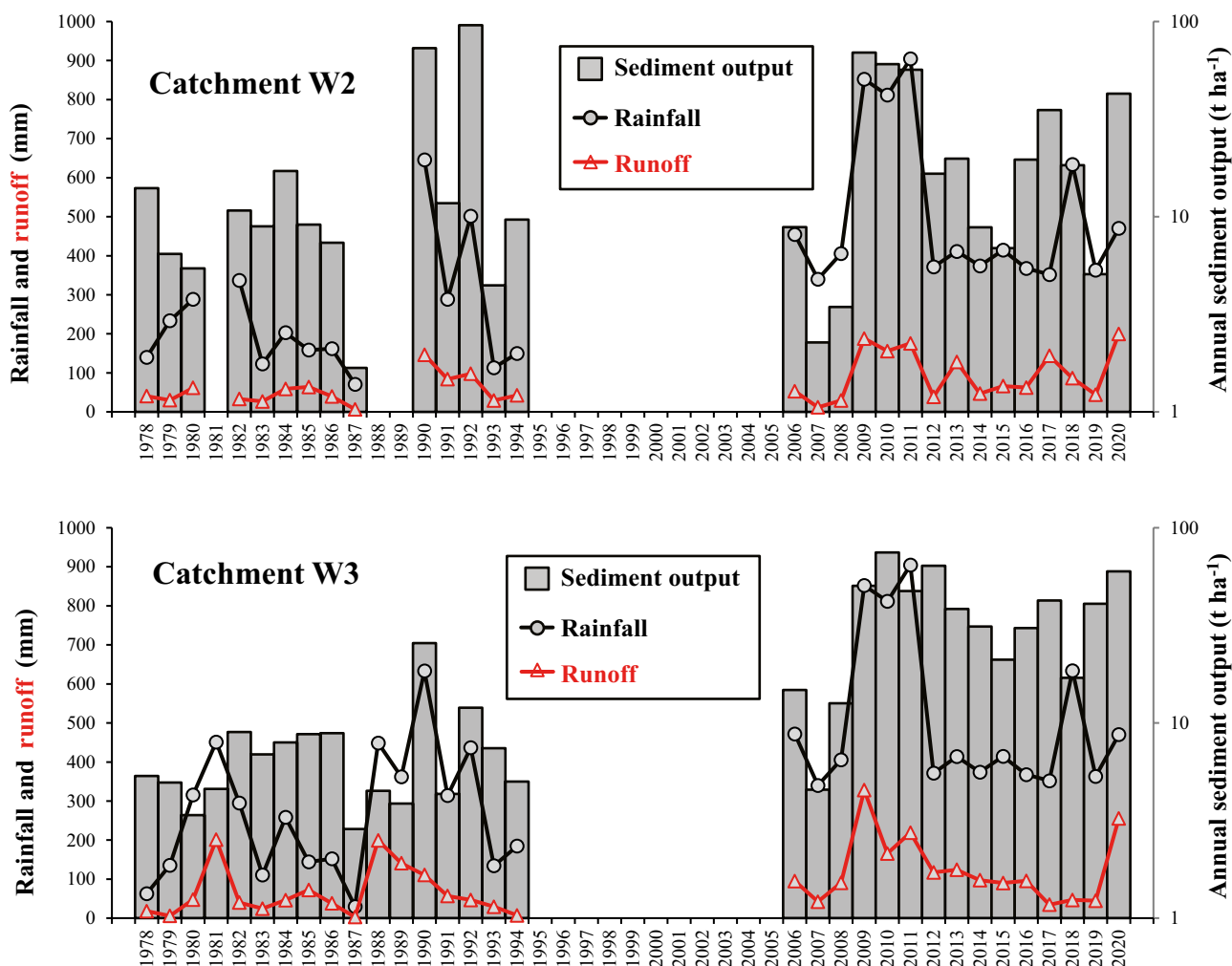
Fig. 3 The annual values of sediment yield and the corresponding measurements of rainfall and runoff obtained from the study catchments W2 and W3

reflect the cutting operation made in 1990 in this catchment whilst the high values obtained in 2009, 2010, 2011 and 2020 in both catchments are mainly associated with flash floods that occurred in those years.

3.2 The ^{137}Cs inventory in the reference area and within the catchments W2 and W3

The application of the ^{137}Cs technique required the comparison of the ^{137}Cs inventories within the two catchments with those obtained in the reference area. The total ^{137}Cs inventories associated with the 12 sectioned cores collected from the reference area in March 2021 are reported in Table 1. The mean value (1623 Bq m^{-2}) calculated from the 12 inventories in Table 1 is consistent with those obtained from the past campaigns in which values ranging between 1565 Bq m^{-2} and 1611 Bq m^{-2} were found (see Porto et al. 2001, 2003a, 2018). The measurements show

a range between 1363 Bq m^{-2} and 1976 Bq m^{-2} with a SD of 187.9 Bq m^{-2} and a CV of 11.9% that reflects the uncertainty under non-eroded conditions.

The 12 corresponding ^{137}Cs profiles are illustrated in Fig. 4 in which the ^{137}Cs activity (Bq kg^{-1}) is plotted against the corresponding soil mass depth (kg m^{-2}). All profiles conform with those typical of undisturbed sites with a maximum value at the soil surface (Profiles 2, 5, 8, 9 and 10) or a peak a few cm below (Profiles 1, 3, 4, 6, 7, 11 and 12).

An uncertainty of approximately 10% at the 95% level of confidence has been associated with the 12 inventory values. Independent measurements of sediment yield are also reported for each catchment.

The values of ^{137}Cs inventory obtained for the 55 bulk cores collected within the catchment W2 ranged from 29 to 1157 Bq m^{-2}, with a mean of 355 Bq m^{-2} and a standard deviation of 306 Bq m^{-2}. All values of ^{137}Cs inventory obtained from these cores are less than the local reference

Table 1 ^{137}Cs inventory values and corresponding erosion rates obtained from the comparison between the inventory values obtained from the sampling sites in the catchments with the inventory values obtained from the 12 sectioned cores collected in the reference site

Profile #	Total inventory (decay-corrected 2020) (Bq m^{-2})	Erosion rate (1954–2020) (t ha^{-1} yr^{-1})		Sediment yield (1978–2020) (t ha^{-1} yr^{-1})	
		W2	W3	W2	W3
1	1593 ± 159	22.3	20.8		
2	1724 ± 172	20.6	19.3		
3	1363 ± 136	15.9	14.6		
4	1747 ± 175	23.4	21.9		
5	1440 ± 144	15.6	13.6		
6	1397 ± 140	20.9	19.0		
7	1717 ± 172	22.7	21.4		
8	1781 ± 178	22.3	21.1		
9	1732 ± 173	19.3	17.9		
10	1578 ± 159	18.2	16.9		
11	1430 ± 143	20.5	19.2		
12	1976 ± 198	23.6	22.4		
Mean	1623	20.4	19.0	22.4 ± 9.3	21.0 ± 7.3
SD	187.9	2.7	2.8		
CV (%)	11.6	13.3	14.8		

inventories reported in Table 1. The general depletion of ^{137}Cs inventory suggests that the catchment W2 has been dominated by net soil loss over the period covered by the ^{137}Cs measurements (i.e. 1954–2020) and that the presence of depositional areas is limited even if local accumulation phenomena cannot be excluded at the scale of single events (Porto and Callegari 2021).

The values of ^{137}Cs inventory obtained for the 81 bulk cores collected within the catchment W3 ranged from 34 to 1559 Bq m^{-2}, with a mean of 405 Bq m^{-2} and a standard deviation of 353 Bq m^{-2}. For this catchment, all values of ^{137}Cs inventory, with the exception of one sampling point, are less than the local reference inventories reported in Table 1. This suggests that even the catchment W3 has been dominated by net soil loss over the period covered by the ^{137}Cs measurements (i.e. 1954–2020).

In Fig. 4, the ^{137}Cs depth distribution obtained from two sectioned cores collected in the catchment area of W2 and W3 is also reported. The ^{137}Cs inventories associated with these depth profiles are 330 Bq m^{-2} and 363 Bq m^{-2}, respectively, for W2 and W3, and are substantially less than the reference inventory. These reduced inventories are therefore indicative of significant soil loss over the period since the commencement of fallout for both catchments. This is further confirmed by the shape of each ^{137}Cs depth profile, which could be seen as reflecting the removal of the surface horizon from the profiles of the reference area shown in Fig. 4.

## 3.3 The relationship between ^{137}Cs loss and sediment yield for the selected events

The main assumption associated with the use of conversion models, able to convert the reduction of ^{137}Cs inventory into estimates of soil erosion rate, is based on a direct relationship between the amount of ^{137}Cs removed from soil and the magnitude of soil erosion. Before the application of the DMM, it was necessary to test the validity of this assumption by comparing the ^{137}Cs loss with the sediment yield for 46 events collected during the period 2013–2021. The values of sediment yield range from 0.04 to 40.5 t ha^{-1} (with a mean value of 3.47 t ha^{-1}) for catchment W2, and from 0.01 to 53.8 t ha^{-1} (with a mean value of 6.25 t ha^{-1}) for catchment W3. The values of ^{137}Cs activity in sediments ranged from 0.1 to 3.8 Bq kg^{-1} with a mean value of 1.2 Bq kg^{-1} for catchment W2, and from 0.6 to 6.4 Bq kg^{-1} with a mean value of 2.3 Bq kg^{-1} for catchment W3. These values were converted into Bq m^{-2} by multiplying the activity times the related mass divided by the catchment area. The final relationship between ^{137}Cs loss (Y_i; Bq ha^{-1}) and sediment yield (X_i; t ha^{-1}) is illustrated in Fig. 5 for the two catchments.

In both cases, a clear statistically significant relationship ($R^2 = 0.80$, for catchment W2, and $R^2 = 0.88$, for catchment W3) is evident and indicates that radionuclide loss and sediment yield are closely related. This direct positive relationship confirms, for both catchments, the basic assumption associated with the ^{137}Cs conversion models used to estimate soil loss (t ha^{-1} yr^{-1}) from the degree of reduction of the ^{137}Cs inventory (i.e. the greater the soil loss, the greater the ^{137}Cs loss).

## 3.4 The particle size composition of soils and sediment

Information on the grain size distributions of the sediment eroded during the 46 individual events and the grain size distributions of the surface soil for the two catchments is provided in Fig. 6. This figure shows a comparison of the frequency distributions of specific surface area (*SSA*) values associated with the sediment samples ($n = 46$) and the samples of surface soil collected at different depth (0–1 cm and 1–15 cm) within each catchment ($n = 55$ for W2 and n = 81 for W3). It is clear from Fig. 6 that, for both catchments, the sediment is generally finer than that of the surface soil (0–1 cm), even if the enrichment in fine fraction is less marked for catchment W3 than for W2.

However, if the deeper (1–15 cm) soil layer is considered, the particle size analysis revealed that the texture of the latter is generally finer than that corresponding to the surface soil (0–1 cm). This is well documented in Fig. 6, in which the frequency distributions of specific surface area
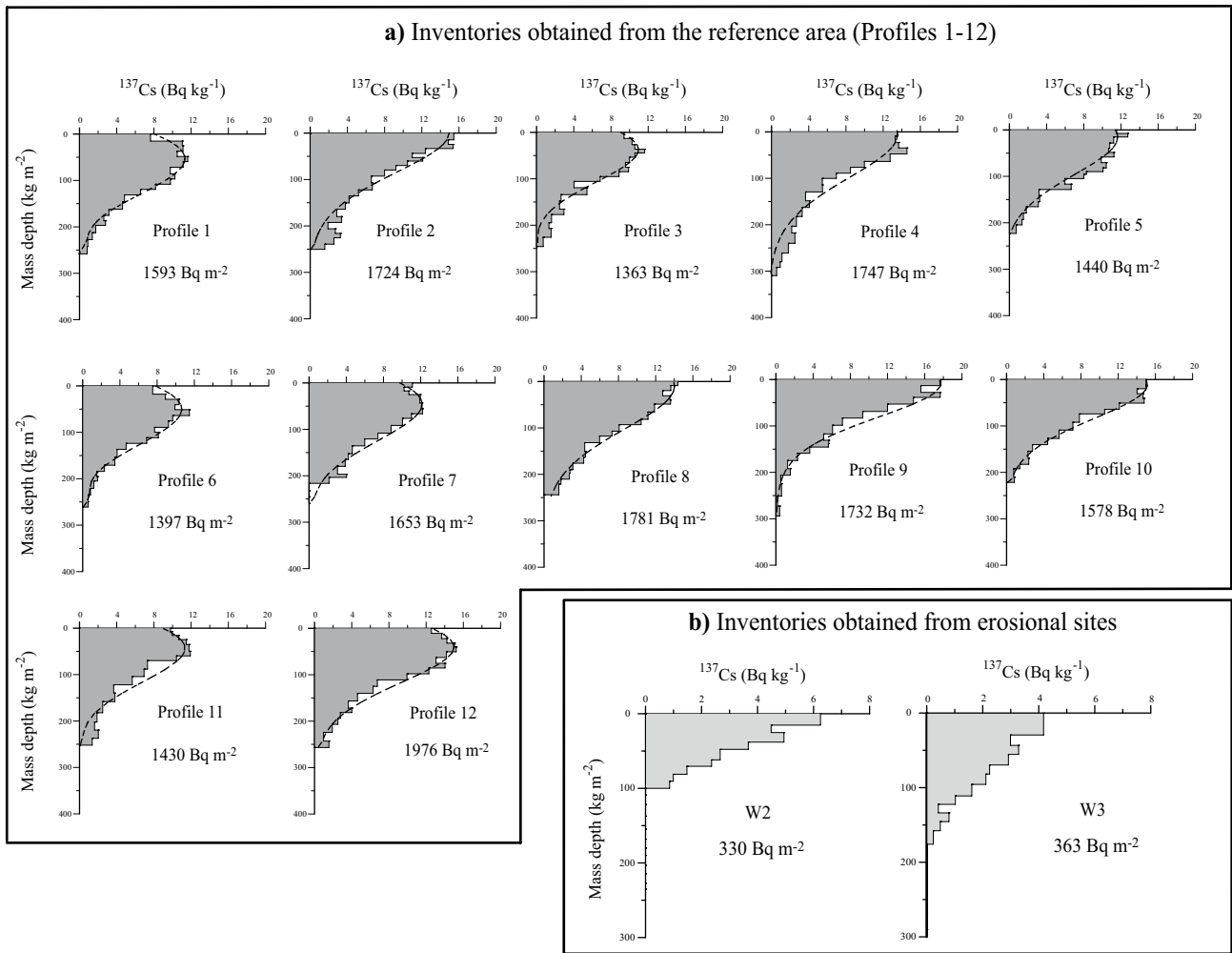
Fig. 4 ^{137}Cs depth distribution associated with **a** the 12 profiles collected from the reference area (the dashed line indicates the simulation obtained with the diffusion and migration model DMM) and **b** the two profiles (indicative of erosional sites) collected within the catchments W2 and W3
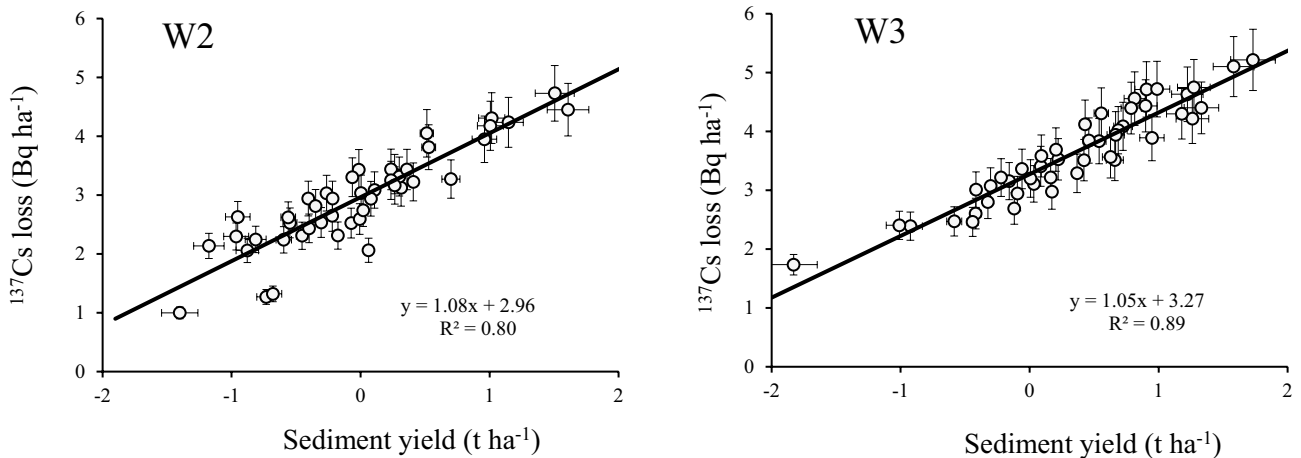
Fig. 5 Relationships between event-based ^{137}Cs loss and sediment yield for the two study catchments. Both *x*- and *y*-axes are expressed in a log-scale to account for the different magnitude of the measurements and to facilitate visualisation of the error bars (±10% to account radiometric uncertainty)
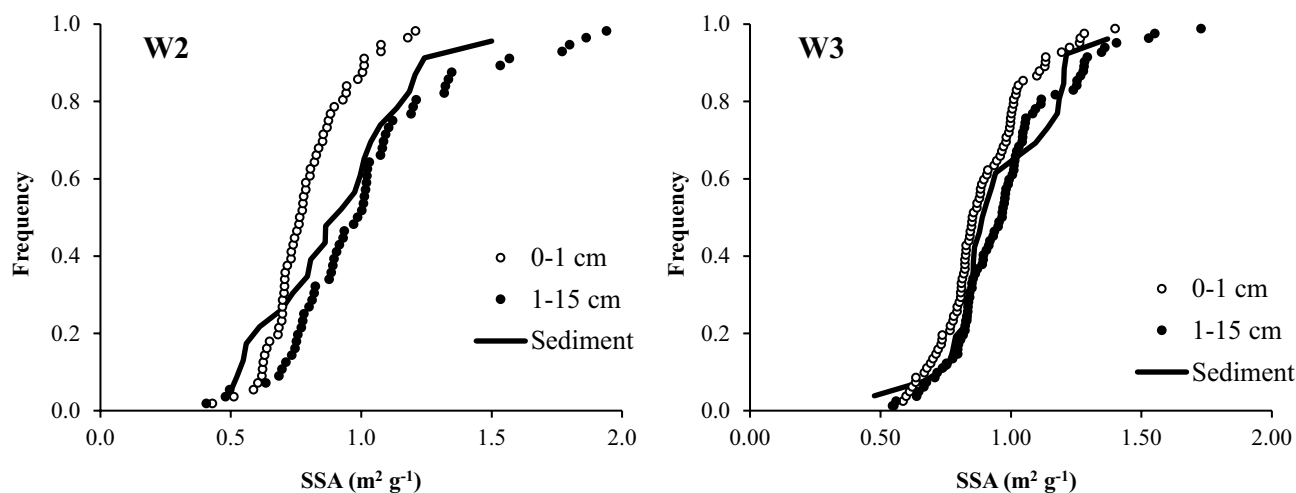
Fig. 6 Comparisons of the frequency distributions of specific surface area (*SSA*) values associated with the sediment samples (*n* = 46) and the samples of surface soil (0–1 cm) and deeper soil layer (1–15 cm) collected within each catchment (*n* = 55 for W2 and *n* = 81 for W3)

(*SSA*) values obtained for the deeper soil layer (1–15) are also superimposed.

## 3.5 The ^{137}Cs activity in mobilised sediment and surface soil

The relationship between the ^{137}Cs activity of mobilised sediment and that in the surface soil is illustrated in Fig. 7, in which the frequency distributions of ^{137}Cs activity values obtained for the sediment samples (*n* = 46 for each catchment) and for the surface soil samples (0–1 cm) collected from each catchment (*n* = 55 for W2 and *n* = 81 for W3) are compared.

4 Discussion

The overall results obtained in this investigation provide important recommendations for the application of the ^{137}Cs technique based on the use of theoretical conversion models. These can be summarised as follows. A first important

recommendation is related to the basic assumption associated with the use of the ^{137}Cs technique that suggests the existence of a close relationship between radionuclide loss and soil loss. The results reported in Fig. 5 provide this first validation because they indicate a significant relationship between ^{137}Cs loss and sediment yield for the 46 events considered in this work. These results are consistent with those obtained in a previous investigation made by Porto et al. (2012) in the same catchments. In that case, 50 different events, related to the period 2005–2011, were analysed and similar relationships between ^{137}Cs loss and soil loss were found. More specifically, significant values of R^2, equal to 0.87 for catchment W2 and to 0.85 for catchment W3, were obtained and these resulted very close with those reported in Fig. 5. Similar results are also available in the literature at plot scale. For example, Porto et al. (2003b), analysing 16 individual events collected over nine experimental plots in Southern Italy, found a simple linear relationship between soil loss and ^{137}Cs loss. Similar findings were also obtained by Porto and Walling (2012) for five cultivated plots located

Fig. 7 Comparison of the frequency distributions of.^{137}Cs activity values associated with the sediment samples (*n* = 46) and the samples of surface soil collected from the two catchments (*n* = 55 for W2 and *n* = 81 for W3)
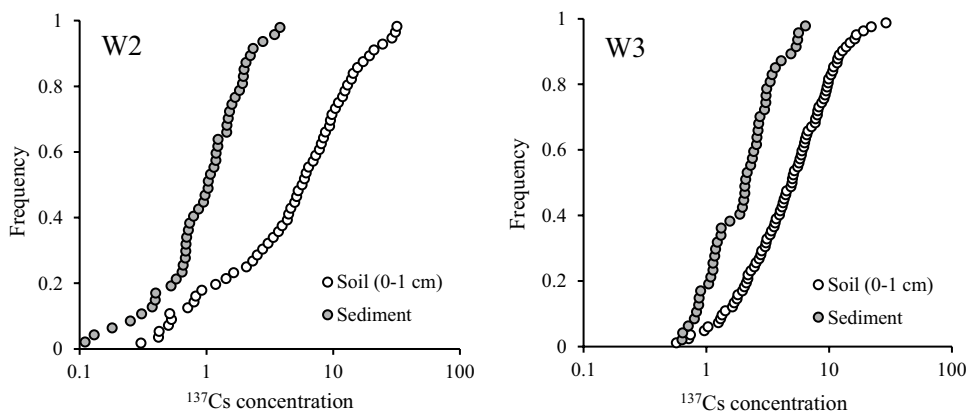
in a different area in Southern Italy. In that case, 57 events were considered and a significant linear relationship between ^{137}Cs loss and soil loss was again observed for each plot.

A second important recommendation is related to the interpretation of the results presented in Fig. 5. They indicate also that there is no clear trend for ^{137}Cs activity in sediment (Y_i) to change as the magnitude of the soil loss (X_i) increases or decreases, because the slope of the regression line, superimposed on the graphs, is essentially close to unity for both catchments. This concept is confirmed by Fig. 8 that shows the relationships between the values of ^{137}Cs activity of sediment samples related to the 46 events and the corresponding values of sediment yield for the two study catchments. At a first sight, these results seem to be contrasting with what could be expected from uncultivated soils. In fact, as documented by Fig. 4, the activity of ^{137}Cs in soil shows a decline when soil depth increases and, consequently, the ^{137}Cs concentration in sediment should decline as well as the magnitude of soil loss increases. Another unexpected result can be deduced when the information reported in Figs. 6 and 7 is combined. Figure 6 shows a general tendency for the eroded sediment to be enriched in fines, suggesting a grain size selectivity of soil loss. This would suggest also that ^{137}Cs concentration in sediment should be higher than that in soil, assuming that ^{137}Cs is preferably associated with the finer fraction (Stone and Walling 1997), but Fig. 7 shows the opposite. These results can be explained only if particle size selectivity and ^{137}Cs activity in soil and sediment are interpreted at catchment scale, in which the variability of texture, soil depletion and ^{137}Cs activity is combined. The results reported in Fig. 6 indicate that, for both catchments, the SSA values of sediment plot closer to those associated with the deeper soil depth (1–15 cm). This would suggest that the enrichment in fine is related not only to a grain size selectivity of soil loss

but also to a preferential association with eroding areas on the catchment (rills or bare areas) in which soil texture is finer. Because these areas are characterised by lower ^{137}Cs concentrations, this assumption seems to provide a first explanation why, as documented in Fig. 7,^{137}Cs concentration in sediment is lower than that in surface soil (0–1 cm). This would also explain the absence of correlation between ^{137}Cs activity in the sediment and the magnitude of sediment yield reported in Fig. 8 for both catchments.

In fact, higher magnitude events are generally associated with an increase in the catchment contributing area and this causes sediment to be mobilised from interrill areas which are characterised by higher ^{137}Cs activity. This effect could be counter-balanced by the mobilisation of sediment from rills or bare areas, in which the deeper soil associated with lower ^{137}Cs concentrations is exposed to erosion. In similar situations, it is difficult to separate the effect due to grain size selectivity of soil loss (sediment enrichment in fine but with higher ^{137}Cs concentrations) from that caused by the occurrence of rill erosion (finer particles eroded from deeper soil layers but with lower ^{137}Cs concentrations) because the first effect may be overridden by the second one. The above considerations may complicate the application of theoretical ^{137}Cs conversion models if the choice of a particle size correction is required. Several authors have in fact emphasised the opportunity to associate the grain size selectivity of erosion processes to a particle size correction factor when ^{137}Cs measurements need to be converted into estimate of soil erosion rates (e.g. Walling and Quine 1990; Sutherland 1991; Walling and He 1999). He and Walling (1996) suggested to incorporate into the conversion models a correction factor P, defined as the ratio of the ^{137}Cs concentration in sediment to that in the original soil, and proposed to estimate it using the following equation that compares the specific surface area of the sediment (SSA_{sed}) with that of the surface soil (SSA_{soil}):
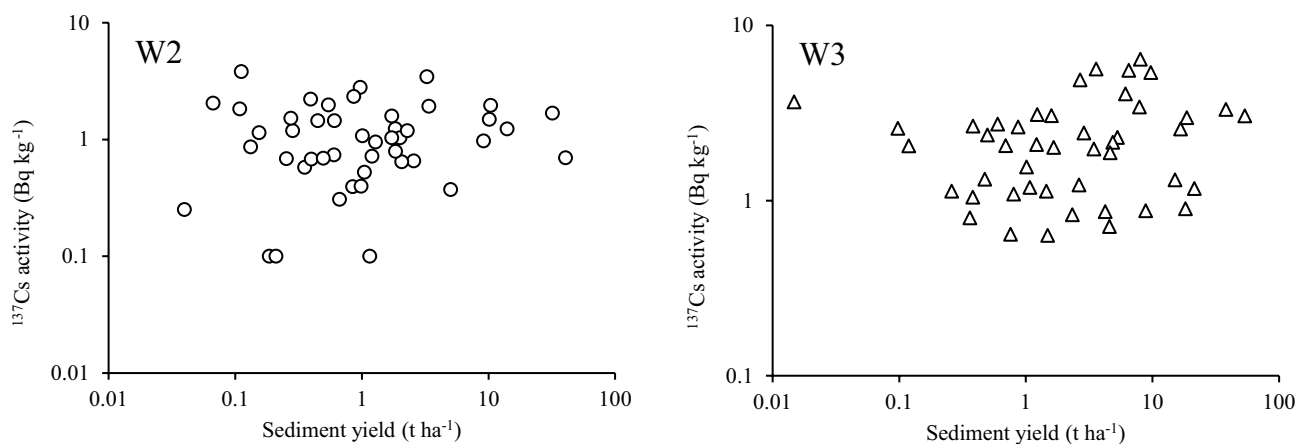

Fig. 8 Relationships between values of ^{137}Cs concentration of sediment samples related to the 46 events and corresponding values of sediment yield for the two study catchments

$$P = \left(\frac{SSA_{sed}}{SSA_{soil}} \right)^{c} \qquad (4)$$

in which the exponent c assumes values ranging from 0.65 to 0.75 (He and Walling 1996).

Equation (4) is plotted in Fig. 9 together with the relationship between the ^{137}Cs enrichment ratio and the specific surface area (SSA) enrichment ratio for both catchments.

A first indication deduced from Fig. 9 suggests that there is no clear evidence of a contrast between the two catchments in terms of the enrichment of sediment relative to soil in either particle size or ^{137}Cs activity. A second, important, finding is related to the plotting position of Eq. (4) that overestimates systematically the SSA enrichment ratio and suggests that the latter cannot be a good indicator to derive P in these catchments. These findings have also important consequences if Eq. (4) is used for particle size correction in similar situations because an overestimation of the P factor will result in an underestimation of soil erosion if the former will be incorporated into a conversion model. Previous works (e.g. Smith and Blake 2014; Foucher et al. 2015; Laceby et al. 2017) have emphasised that even if fallout radionuclides are enriched in fine particle size fractions their relationships with SSA may be contrasting depending on the sources. As mentioned above, the depth-dependent (decreasing) distribution of ^{137}Cs in the soil profile relates to the exposure to fallout, and therefore, its concentration may decrease with soil depth despite an increasing clay content documented by our measurements. For the above reasons, in the absence of empirical methods able to provide suitable estimates of P, and because of the overall particle size balancing due to the mobilisation of sediment from areas with different combination of ^{137}Cs activity and
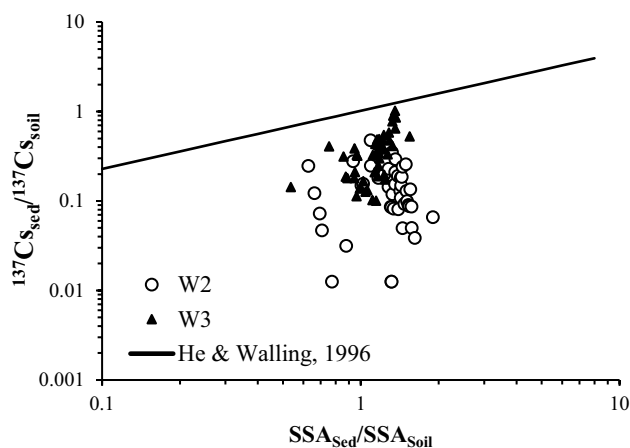
Fig. 9 Comparison between the ^{137}Cs enrichment ratio and the specific surface area ratio for the sediments collected from the catchment W2 and W3 during the 46 events. The relationship proposed by He and Walling (1996) has been superimposed

texture, we decided to neglect the effect of particle size in our conversion model and we assumed the value of $P = 1$ to estimate soil erosion rates from ^{137}Cs measurements in our catchments.

A third important suggestion is related to the spatial variability of the ^{137}Cs fallout both in the reference area and within the study catchments and to the need to incorporate this uncertainty into the theoretical conversion model. This problem was already subject of investigation in previous papers made by the authors (Porto et al. 2014, 2018, 2022). The first source of uncertainty is related to the temporal and spatial variability of the ^{137}Cs fallout in the reference area. In a recent investigation, Porto and Callegari (2022) made an attempt to reconstruct the temporal fallout in the area by using the 12 sampling points reported in Fig. 1 together with the temporal fallout record provided at national scale (see ISIN 2021). The overall results revealed the presence of a Chernobyl component in the study area that accounts, on average, for approximately 25% of the total fallout. This additional component was incorporated into the DMM and each single value of the 12 reference inventories reported in Table 1 was used independently to provide the final estimates of soil erosion. This strategy allowed to treat the erosion rates obtained from the ^{137}Cs measurements as a range instead of a single mean value and this provided evidence of the uncertainty associated with the spatial variability in the reference area. The second source of uncertainty is related to the spatial variability of the ^{137}Cs fallout within the catchments in which the presence of trees may have affected the amount of radionuclide that reached the ground. Several studies have emphasised this effect (e.g. Bunzl et al. 1995; Takenaka et al. 1998; Strebl et al. 1999). As we said above, our samples were collected from small clearings under the trees and two bulk cores were taken for each sampling point to reduce this effect. However, it is important to emphasise that the eucalyptus trees were planted in 1968 and these trees did not reach maturity before 4–5 years after planting. Prior to 1973, most of ^{137}Cs fallout had already reached the ground and at that time, the ground was similar to that of the undisturbed area selected as reference site. As a result, in these two catchments, fallout interception was minimal during the period covered by the trees and the ^{137}Cs inventories are then comparable with those obtained in the reference area.

Taking into account all the above indications, it was possible to apply the DMM, described by Eqs. (1) and (3), in which these sources of uncertainty were incorporated. Its application required the integration of Eq. (3) over mass depth x that will give the total ^{137}Cs inventory A_u (Bq m^{-2}) for an erosion site at time t:

$$A_u(t) = \int_0^\infty PC(x,t)dx \qquad (5)$$

and could be used to get the estimate of soil erosion rates from each sampling point. Equation (5) includes the parameter P, defined as before, that, for this specific case, was set equal to 1, and the temporal distribution of ^{137}Cs fallout reconstructed for this area (Porto and Callegari 2022). Equations (1), (3) and (5) were solved simultaneously for E (kg m^{-2}), by replacing A_u (Bq m^{-2}) with the measured inventory related to an eroding point. Erosion rates R (kg m^{-2} yr^{-1}) may then be obtained by dividing the quantity E by the time $t - t_0$ (year) elapsed from the commencement of ^{137}Cs fallout (Parson 1954) to the date of sampling. The ability of DMM to reproduce the experimental ^{137}Cs distribution along the soil profile is confirmed in Fig. 4, in which the dashed line representing the model is superimposed on each experimental profile obtained in this work. The results of this application exercise are reported in Table 1, in which the value of erosion rate corresponding to each profile represents the average of the erosion rates obtained for the 55 sampling points in the catchment W2 and for the 81 sampling points in the catchment W3. In order to facilitate interpretation, the results reported in Table 1 were presented graphically in Fig. 10, in which the comparison between this range of estimates with the range of sediment yield measurements is reported.

It is worthy noticing that, as indicated above, there is no evidence of significant deposition within the catchments because all the Cs-137 inventories in the catchments are lower than the reference value. In similar cases, when the catchment area is small and long-term measurements are considered, Playfair's law of stream morphology (Boyce 1975) establishes that over a long time a stream must essentially transport all sediment delivered from the hillslopes to it. For this reason a sediment delivery ratio (SDR) close to 1.0 can be assumed. This comparison required also the opportunity to treat even the measurements of sediment yield as a range instead of a single mean value by taking into account their temporal variability related to the occurrence of flash floods and silvicultural treatments. We accounted for this uncertainty by expressing the measurements as a range around the central value (given by the average and its uncertainty assumed at the 95% level of confidence, i.e. ± 2 SE).

It is clear from Table 1 and Fig. 10 that the mean values of sediment yield measured in both catchments during the monitoring period (from 1978 to 2020) fall within the range covered by the estimates of net erosion provided by the ^{137}Cs measurements. We are confident that the slight difference between soil erosion estimates (via ^{137}Cs) and measured sediment yield is related mainly to the different time span associated to the datasets. The erosion rates derived from ^{137}Cs measurements are related to a longer time window (1954–2020) whilst the measurements of sediment yield cover the period 1978–2020. It is likely that during the last 3–4 decades climate change affected sediment yield and, as a consequence, our measurements of sediment yield could be a little higher than those that have occurred prior to the monitoring period.

Fig. 10 Comparison between net erosion rates provided by ^{137}Cs measurements and values of sediment yield for the two study catchments
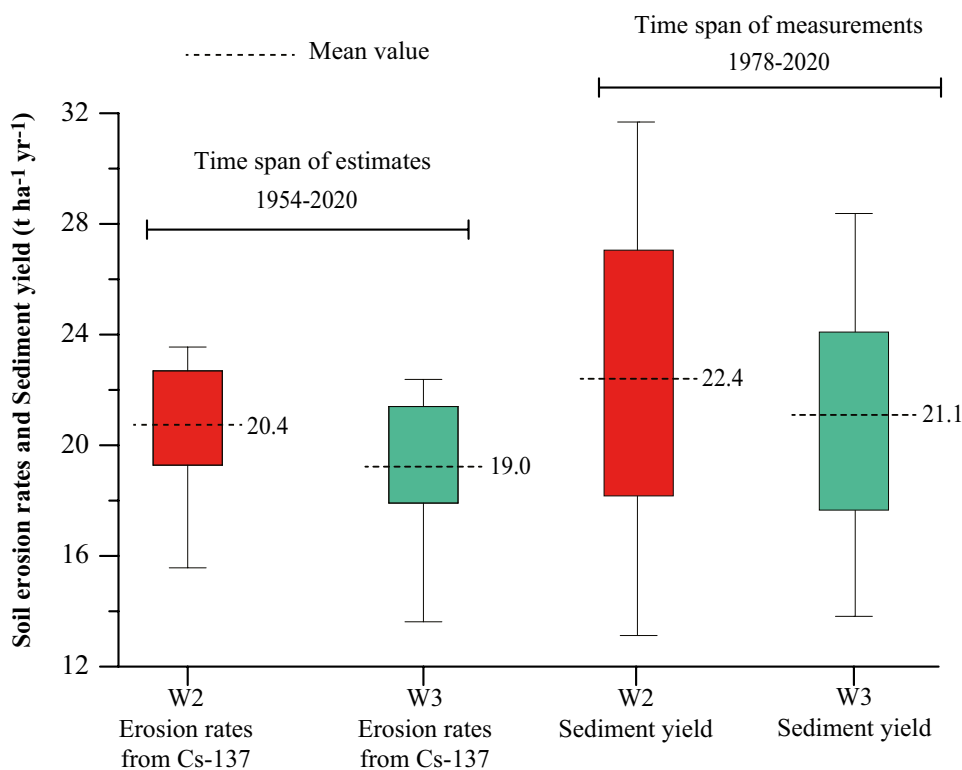
However, the overall results indicate that, for the catchments investigated in this work, there is no reason to assume that a value of the P factor differed from 1, if a long-term estimate of soil erosion is required.

These findings suggest also that the ^{137}Cs technique, if some of the uncertainties associated with the measurements are incorporated into the conversion models, is a useful means to provide soil erosion estimates in the absence of other methods.

5 Conclusions

A long-term monitoring programme, which involves the use of two experimental catchments in Southern Italy, provided important information on the ability of the ^{137}Cs technique to estimate soil erosion rates in this geographic area. The work reported here revealed, preliminarily, that some of the basic assumptions made by the use of this technique can be validated if direct long-term observations of sediment yield are available. In this respect, a clear significant relationship between radionuclide loss and sediment yield has been documented for 46 events available for the study catchments and it provided a first validation test. Secondly, some of the uncertainties associated with the spatial and temporal variability of ^{137}Cs fallout were considered and incorporated into the conversion model DDM. This uncertainty was accounted by a specific investigation made on the reference area for which 12 ^{137}Cs profiles were considered. Thirdly, detailed information on particle size and ^{137}Cs concentration in both sediments and soils allowed to establish that sediment characteristics may be considered as a result of a combination between rill and interrill erosion processes. In other words, the nature of sediment transport, especially related to cohesive soils as for our catchments, is a very complex process that depends on density, aggregate stability and grain size. This process is complicated further by the ^{137}Cs depth-dependent distribution (decreasing with depth). These findings suggest that traditional relationships used to account for particle size effects may not be dependent only on soil and sediment texture. For this reason, the calibration parameter P incorporated into the conversion model cannot be estimated using the SSA enrichment ratio and could be assumed equal to 1 in the absence of reliable methods. Based on our datasets of sediment yield, available for the two study catchments W2 and W3, the Diffusion and Migration Model (DMM), if no corrections for particle size effect are taken into account, proved to be an effective means to derive long-term estimates of soil erosion rate. Its performance was confirmed by a close agreement between these estimates and the independent measurements of sediment yield for the study catchments. However, further work is necessary to confirm further these results in different geomorphic contexts where long-term measurements of soil erosion or sediment yield are available.

Declarations

References

Altieri V, De Franco S, Lombardi F, Marziliano PA, Menguzzato G, Porto P (2018) The role of silvicultural systems and forest types in preventing soil erosion processes in mountain forests. A methodological approach using Caesium-137 measurements. J Soils Sediments 18(12):3378–3387

Barsanti M, Conte F, Delbono I, Iurlaro G, Battisti P, Bortoluzzi S, Lorenzelli R, Salvi S, Zicari S, Papucci C, Delfanti R (2012) Environmental radioactivity analyses in Italy following the Fukushima Dai-ichi nuclear accident. J Environ Radioactiv 114:126–130

Belyaev VR, Golosov VN, Markelov MV, Evrard O, Ivanova NN, Paramonova TA, Shamshurina EN (2013) Using Chernobyl-derived ^{137}Cs to document recent sediment deposition rates on the River Plava floodplain (Central European Russia). Hydrol Process 27:807–821

Boyce RC (1975) Sediment routing with sediment delivery ratios. Present and prospective technology for predicting sediment yield and sources, Publ. ARS-S-40, U.S. Department of Agriculture, Washington, D.C.:61–65

Brakensiek DL, Osborn HB, Sheridan JM (1979) Field manual for research in agricultural hydrology. Agriculture Handbook no. 224 (US Department of Agriculture Science and Education Administration, Washington)

Bunzl K, Kracke W, Schimmack W (1995) Migration of fallout $^{239+240}Pu$, ^{241}Am and ^{137}Cs in the various horizons of a forest soil under pine. J Environ Radioactiv 28:17–34

Campbell BL, Loughran RJ, Elliott GL (1988) A method for determining sediment budget using caesium-137. IAHS Publ 174:171–179

Carter CE, Parson DA (1967) Field tests on the Coshoctontype wheel runoff sampler. Trans Am Soc Agric Eng 10(1):133–135

Cerdan O, Govers G, Le Bissonnais Y, Van Oost K, Poesen J, Saby N, Gobin A, Vacca A, Quinton J, Auerswald K, Klik A, Kwaad FJPM, Raclot D, Ionita I, Rejman J, Rousseva S, Muxart T, Roxo MJ, Dostal T (2010) Rates and spatial variations of soil erosion in Europe: a study based on erosion plot data. Geomorphology 122:167–177

Crank J (1975) The mathematics of diffusion. 2nd ed. Clarendon Press, pp. 414

Di Stefano C, Ferro V, Porto P, Rizzo S (2005) Testing a spatially distributed sediment delivery model (SEDD) in a forested basin by caesium-137 technique. J Soil Water Conserv 60(3):148–157

Elliott GL, Campbell BL, Loughran RJ (1990) The correlation of erosion measurement and soil caesium-137 content. Appl Radiat Isot 41:713–717

Estrany J, Lopez-Tarazon JA, Smith HG (2016) Wildfire effects on suspended sediment delivery quantified using fallout radionuclide tracers in a Mediterranean catchment. Land Degrad Dev 27:1501–1512

Foucher A, Laceby PJ, Salvador-Blanes S, Evrard O, Le Gall M, Lefèvre I, Cerdan O, Rajkumar V, Desmet M (2015) Quantifying the dominant sources of sediment in a drained lowland agricultural catchment: the application of a thorium-based particle size correction in sediment fingerprinting. Geomorphology 250(1):271–281

He Q, Walling DE (1996) Interpreting particle size effects in the adsorption of ^{137}Cs and unsupported ^{210}Pb by mineral soils and sediments. J Environ Radioact 30(2):117–137

He Q, Walling DE (1997) The distribution of fallout ^{137}Cs and ^{210}Pb in undisturbed and cultivated soils. Appl Radiat Isot 48:677–690

Heywood MJT, Walling DE (2007) The sedimentation of salmonid spawning gravels in the Hampshire Avon catchment, UK: implications for the dissolved oxygen content of intragravel water and embryo survival. Hydrol Process 21:770–788

International Atomic Energy Agency (2014) Guidelines for using fallout radionuclides to assess erosion and effectiveness of soil conservation strategies. IAEA-TECDOC-1741. IAEA, Vienna

ISIN (2021) Attività nucleari e radioattività ambientale. Rapporto ISIN sugli indicatori. II edizione 2021 - Dati 2020. Ispettorato nazionale per la sicurezza nucleare e la radioprotezione (in Italian)

Kachanoski RG (1987) Comparison of measured soil 137-Cesium losses and erosion rates. Can J Soil Sci 67:199–203

Laceby PJ, Evrard O, Smith HG, Blake WH, Olley JM, Minella JPG, Owens PN (2017) The challenges and opportunities of addressing particle size effects in sediment source fingerprinting: a review. Earth-Sci Rev 169:85–103

Li S, Lobb DA, Tiessen KHD, McConkey BG (2010) Selecting and applying ^{137}Cs conversion models to estimate soil erosion rates in cultivated fields. J Environ Qual 39:204–219

Lindstrom FT, Boersma L (1971) A theory on the mass transport of previously distributed chemicals in a water-saturated sorbing porous medium. Soil Sci 111:192–199

Lobb DA, Kachanoski RG, Miller MH (1995) Tillage translocation and tillage erosion on shoulder slope landscape positions measured using ^{137}Cs as a tracer. Can J Soil Sci 75:211–218

Loughran RJ, Campbell BL (1995) The identification of catchment sediment sources. In: Foster IDL, Gurnell AM, Webb B (eds) Sediment and Water Quality in River Catchments. Wiley, Chichester, pp 189–206

Mabit L, Benmansour M, Walling DE (2008) Comparative advantages and limitations of the fallout radionuclides ^{137}Cs, ^{210}Pb$_{ex}$ and ^{7}Be for assessing soil erosion and sedimentation. J Environ Radioactiv 99:1799–1807. https://doi.org/10.1016/j.jenvrad.2008.08.009

Mabit L, Blake WH (eds.) (2019) Assessing recent soil erosion rates through the use of beryllium-7 (Be-7). Springer Nature Switzerland AG

Mabit L, Klik A, Benmansour M, Toloza A, Geisler A, Gerstmann UC (2009) Assessment of erosion and deposition rates within an Austrian agricultural watershed by combining ^{137}Cs, ^{210}Pb$_{ex}$ and conventional measurements. Geoderma 150(3–4):231–239

Maetens W, Poesen J, Vanmaercke M (2012) How effective are soil conservation techniques in reducing plot runoff and soil loss in Europe and the Mediterranean? Earth-Sci Rev 115:21–36

Manojlović S, Antić M, Šantić D, Sibinović M, Carević I, Srejić T (2018) Anthropogenic impact on erosion intensity: case study of rural areas of Pirot and Dimitrovgrad municipalities, Serbia. Sustainability 10:826

Minella JPG, Walling DE, Merten GH (2014) Establishing a sediment budget for a small agricultural catchment in Southern Brazil, to support the development of effective sediment management strategies. J Hydrol 519:2189–2201

Moustakim M, Benmansour M, Zouagui A, Nouira A, Benkdad A, Damnati B (2019) Use of caesium-137 re-sampling and excess lead-210 techniques to assess changes in soil redistribution rates within an agricultural field in Nakhla watershed. J Afr Earth Sci 156:158–167

Navas A, López-Vicente M, Gaspar L, Palazón L, Quijano L (2014) Establishing a tracer based sediment budget to preserve wetlands in Mediterranean mountain agroecosystems (NE Spain). Sci Total Environ 496:132–143

Nearing MA, Xie Y, Liu B, Ye Y (2017) Natural and anthropogenic rates of soil erosion. Int Soil Water Conservat Res 5(2):77–84

Owens PN, Blake WH, Giles TR, Williams ND (2012) Determining the effects of wildfire on sediment sources using ^{137}Cs and unsupported ^{210}Pb: the role of landscape disturbances and driving forces. J Soils Sediments 12:982–994

Panagos P, Standardi G, Borrelli P, Lugato E, Montanarella L, Bosello F (2018) Cost of agricultural productivity loss due to soil erosion in the European Union: from direct cost evaluation approaches to the use of macroeconomic models. Land Degrad Dev. https://doi.org/10.1002/ldr.2879

Parson DA (1954) Coshocton-type runoff samplers, laboratory investigations. U.S. Department of Agriculture, Soil Conservation Service, Washington, D.C

Pegoyev AN, Fridman ShD (1978) Vertical profiles of caesium-137 in soils (English translation). Pochvovedeniye 8:77–81

Porto P, Bacchi M, Preiti G, Romeo M, Monti M (2022) Combining plot measurements and a calibrated RUSLE model to investigate recent changes in soil erosion in upland areas in Southern Italy. J Soils Sediments 22:1010–1022

Porto P, Callegari G (2019) Initial results of sediment yield measurement interpretation using a regional approach: Southern Italy case study. IAHS Publ 381:49–54

Porto P, Callegari G (2021) Using ^{7}Be measurements to explore the performance of the SEDD model to predict sediment yield at event scale. Catena 196:104904

Porto P, Callegari G (2022) Comparing long-term observations of sediment yield with estimates of soil erosion rate based on recent 137Cs measurements. Results from an experimental catchment in Southern Italy. Hydrol Process 36(9):e14663. https://doi.org/10.1002/hyp.14663

Porto P, Walling DE (2012) Validating the use of ^{137}Cs and ^{210}Pb$_{ex}$ measurements to estimate rates of soil loss from cultivated land in southern Italy. J Environ Radioact 106:47–57

Porto P, Walling DE (2015) Use of caesium-137 Measurements and long-term records of sediment load to calibrate the sediment delivery component of the SEDD model and explore scale effect: examples from Southern Italy. J Hydrol Eng. https://doi.org/10.1061/(ASCE)HE.1943-5584.0001058

Porto P, Walling DE, Alewell C, Callegari G, Mabit L, Mallimo N, Meusburger K, Zehringer M (2014) Use of a ^{137}Cs re-sampling technique to investigate temporal changes in soil erosion and sediment mobilisation for a small forested catchment in southern Italy. J Environ Radioact 138:137–148

Porto P, Walling DE, Callegari G (2004) Validating the use of caesium-137 measurements to estimate erosion rates in three small catchments in Southern Italy. IAHS Publ 288:75–83

Porto P, Walling DE, Callegari G (2005) Investigating sediment sources within a small catchment in southern Italy. IAHS Publ 291:113–122

Porto P, Walling DE, Callegari G (2009) Investigating the effects of afforestation on soil erosion and sediment mobilisation in two small catchments in Southern Italy. Catena 79:181–188

Porto P, Walling DE, Callegari G (2018) Using repeated ^{137}Cs and [210]Pb$_{ex}$ measurements to establish sediment budgets for different time windows and explore the effect of connectivity on soil erosion rates in a small experimental catchment in Southern Italy. Land Degrad Dev 29:1819–1832

Porto P, Walling DE, Callegari G, La Spada C (2012) Further investigation of the relationship between ^{137}Cs and [210]Pb$_{ex}$ flux and sediment output from two small experimental catchments in Calabria, southern Italy. IAHS Publ 356:385–393

Porto P, Walling DE, Ferro V (2001) Validating the use of caesium-137 measurements to estimate soil erosion rates in a small drainage basin in Calabria, southern Italy. J Hydrol 248(1):93–108. https://doi.org/10.1016/S0022-1694(01)00389-4

Porto P, Walling DE, Ferro V, Di Stefano C (2003a) Validating erosion rate estimates provided by caesium-137 measurements for two small forested catchments in Calabria, southern Italy. Land Degrad Dev 14:389–408. https://doi.org/10.1002/ldr.561

Porto P, Walling DE, La Spada C, Callegari G (2016) Validating the use of ^{137}Cs measurements to derive the slope component of the sediment budget of a small catchment in southern Italy. Land Degrad Dev 27:798–810

Porto P, Walling DE, Tamburino V, Callegari G (2003b) Relating caesium-137 and soil loss from cultivated land. Catena 53:303–326

Ritchie JC, McHenry JR (1990) Application of radioactive fallout cesium-137 for measuring soil erosion and sediment accumulation rates and patterns: a review. J Environ Qual 19:215–233

Ritchie JC, Ritchie CA (2005) Bibliography of publications of 137-cesium studies related to erosion and sediment deposition. USDA-ARS Hydrology and Remote Sensing Laboratory. Occasional Paper HRSL-2005–01

Romero-Díaz A, Ruiz-Sinoga JD, Robledano-Aymerich F, Brevik EC, Cerdà A (2017) Ecosystem responses to land abandonment in Western Mediterranean Mountains. Catena 149:824–835

Smith HG, Blake WH (2014) Sediment fingerprinting in agricultural catchments: a critical re-examination of source discrimination and data corrections. Geomorphology 204:177–191

Stone PM, Walling DE (1997) Particle size selectivity considerations in sediment budget investigations. Water Air Soil Pollut 99:63–70

Strebl F, Gerzabek MH, Bossew P, Kienzl K (1999) Distribution of radiocaesium in an Austrian forest stand. Sci Total Environ 226:75–83

Sutherland RA (1991) Examination of caesium-137 areal activities in control (uneroded) locations. Soil Technol 4:33–50

Takenaka C, Onda Y, Hamajima Y (1998) Distribution of cesium-137 in Japanese forest soils: correlation with the contents of organic carbon. Sci Total Environ 222:193–199

Taylor A, Blake WH, Keith-Roach MJ (2014) Estimating Be-7 association with soil particle size fractions for erosion and deposition modelling. J Soils Sediments 14:1886–1893

Walling DE, He Q (1998) Use of fallout ^{137}Cs measurements for validating and calibrating soil erosion and sediment delivery models. IAHS Publ 249:267–278

Walling DE, He Q (1999) Improved models for estimating soil erosion rates from cesium-137 measurements. J Environ Qual 28:611–622

Walling DE, Quine TA (1990) Calibration of caesium-137 measurements to provide quantitative erosion rate data. Land Degrad Rehab 2:161–175

Walling DE, Quine TA (1992) The use of caesium-137 measurement in soil erosion surveys. IAHS Publ 210:143–152

Wilkinson SN, Wallbrink PJ, Hancock GJ, Blake WH, Shakesby RA, Doerr SH (2009) Fallout radionuclide tracers identify a switch in sediment sources and transport-limited sediment yield following wildfire in a eucalypt forest. Geomorphology 110(3–4):140–151

Wood PJ, Armitage PD (1999) Sediment deposition in a small lowland stream: management implications. Regul Rivers 15:199–210

Yang H, Chang Q, Du M, Minami K, Hatta T (1998) Quantitative model of soil erosion rates using ^{137}Cs for uncultivated soil. Soil Sci 163:248–257

Young RA (1980) Characteristics of eroded sediment. Trans Am Soc Agric Eng 23(1139–1142):1146

Young RA, Onstad CA (1978) Characterization of rill and interrill eroded soil. Trans Am Soc Agric Eng 21:1126–1130

Zapata F (ed) (2002) Handbook for the assessment of soil erosion and sedimentation using environmental radionuclides. Kluwer, Dordrecht

Zhang XC (2017) Evaluating WEPP hillslope model using ^{137}Cs-derived spatial soil redistribution data. Soil Sci Soc Am J 81:179–188

Zhang XC (2018) Evaluating sediment deposition prediction by three ^{137}Cs erosion conversion models. Soil Sci Soc Am J 82:931–938

Zhang XC, Polyakov VO, Liu BY, Nearing MA (2019) Quantifying geostatistical properties of ^{137}Cs and [210]Pb$_{ex}$ at small scales for improving sampling design and soil erosion estimation. Geoderma 334:155–164

Authors and Affiliations

P. Porto[1,2] · **G. Callegari[2]**

✉ P. Porto
paolo.porto@unirc.it

[1] Dipartimento di Agraria, University Mediterranea of Reggio Calabria, Feo di Vito, Reggio Calabria 89122, Italy

[2] Institute for Agricultural and Forest Systems in the Mediterranean (ISAFOM) - National Research Council (CNR), Via Cavour, 4/6, Rende, CS 87036, Italy